A STRAIN BASED APPROACH TO ASSESSING CREEP CRACK INITIATION AND CRACK GROWTH

D.J. Smith and A.J. Fookes

Department of Mechanical Engineering, University of Bristol, Bristol, BS8 1TR, UK

ABSTRACT

Recently, there has been considerable interest in studying creep crack growth in brittle materials. For example, the methodologies for assessing creep ductile materials, using fracture mechanics parameters like C^* and C_t, have been extended to include creep brittle materials. This paper begins by examining these recent developments and outlines the difficulties in adopting these methods. An alternative approach is then proposed in this paper. This new approach is based on recent work on development of a strain based failure assessment diagram (SBFAD). Experimental results from a series of tests on a simulated heat affected zone of a low alloy steel are examined. It is shown that the results agree well with the analysis using a SBFAD. The application of the methodology for assessing the initiation and growth of a defect in a creep brittle material is demonstrated.

KEYWORDS

Creep brittle, creep crack growth, Strain based failure assessment diagram, material resistance.

INTRODUCTION

Previous research [1-3] on characterising creep crack growth (CCG) has focussed on characterising the rate of creep crack growth in terms of C^*, the creep equivalent of the non-linear fracture parameter J. The bulk of this work has examined creep-ductile materials, in which CCG is accompanied by significant amounts of creep deformation. However, a more problematic class of high-temperature structural materials are creep-brittle materials where the extent of creep deformation is small compared to the total displacement.

In order to allow creep-brittle materials to be assessed using C^* the validity limits in the CCG testing standard [4] have been relaxed [5]. This includes decreasing the amount of creep deformation required and to widen the regime of creep crack extension. Alternatively the C_t parameter has been proposed to characterise CCG for small-scale creep conditions [6]. However, even with the reduction of the limitations there are still a number of observed shortcomings associated with using C^* for characterising creep crack growth. For example, the initial stage of CCG, and the subsequent steady CCG rate [6] cannot be described uniquely by C^*. In brittle alloys this can mean in many cases that

only the latter part of the test (usually less than 50% and sometimes as little as 10% of the remaining life of the test [8]) can be characterised. Consequently it is only the accelerating portion that is uniquely described by C^*. This is demonstrated clearly by [7,9-10]. In this latter stage it has also been suggested that measured values of C^* become equivalent to the CCG rate [11]. This is because, at large CCG rates, most of the displacement rate results from increases in the elastic compliance due to crack extension and not from creep deformation taking place within the specimen. With these concerns in mind this paper examines an alternative approach.

The development of the strain-based failure assessment diagram (SBFAD) is explored, which could potentially simplify the treatment of situations involving variable stress and variable temperature. A ferritic steel representative of the simulated heat affected zone of a low alloy steel is examined at 380°C using the new SBFAD.

STRAIN BASED FAILURE ASSESSMENT DIAGRAM (SBFAD)

A high temperature time dependent failure assessment diagram (TDFAD) based on the well established low temperature R6 approach [12], has been developed which allows predictions of creep initiation time and times for small amounts of CCG [13]. The TDFAD uses a high temperature 'creep toughness' which replaces the fracture toughness used in the R6 procedure. This 'creep toughness' parameter may be examined directly from experimental load-displacement information or indirectly from CCG rates as a function of C*. A strain based failure assessment diagram (SBFAD) has recently been developed as an alternative to the stress based TDFAD for high temperature components [14]. Strain accumulation can be measured or calculated and could be used to provide a measure of the components continuing performance. This section very briefly describes the SBFAD.

The Option 2 FAD in R6 [12] may be extended to described a TDFAD [13] given by

$$K_r = \left[\frac{E\varepsilon_{ref}^T}{L_r\sigma_{0.2}^c} + \frac{L_r^3\sigma_{0.2}^c}{2E\varepsilon_{ref}^T} \right]^{-1/2}$$

(1)

where $K_r = K_{applied}/K_{mat}$, $L_r = \sigma_{ref}/\sigma_{0.2}^c$, ε_r is the reference strain corresponding to the reference stress σ_{ref}, and $\sigma_{0.2}^c$ is the stress at 0.2% strain from the isochronous stress-strain curve. It is possible to recast eqn 1 to give K_r as a function of normalised strain ε_r, where

$$K_r = 1/\sqrt{\left[\varepsilon_r + 0.5L_r^2/\varepsilon_r\right]}$$

(2)

and ε_r is the ratio of the total to elastic strain at reference stress, $\left(\varepsilon_{ref}^T/\varepsilon_{ref}^e\right)$.

For a structure, a relationship between the reference strains and the load line displacements is required. Preliminary studies using the EPRI handbook solutions [15] have shown that for the compact tension (CT) specimen for a/W=0.5 and 0.75, where a is the crack length and W is the specimen width the normalised strain may be related to the load line displacement by

$$\varepsilon_r = \left(\frac{2.4\Delta_T}{\Delta_e} - 1.4\right)$$

(3)

where Δ_T is the total load line displacement and Δ_e is the elastic load line displacement.

Figure 1 shows a schematic SBFAD, with curves for K_r as a function of ε_r for L_r
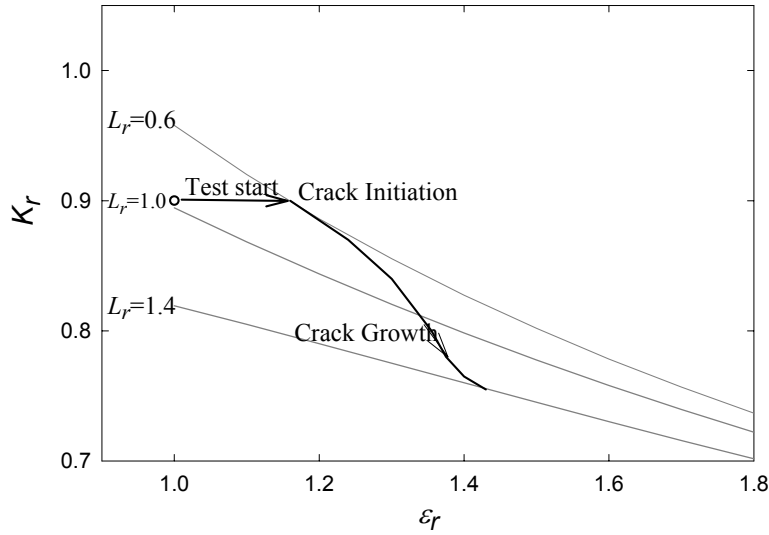
Figure 1, SBFAD Assessment of Creep Crack Growth

varying from 0.6 to 1.4. For large strains the SBFAD is reasonably independent of L_r. Now consider a cracked component subjected to a constant load corresponding to L_r=0.6 and K_r=0.9. At the start of the life (and assuming zero inelastic strain during loading) ε_r=1.0. Creep strain accumulation without crack growth corresponds to a horizontal line in figure 1. Crack initiation is assumed to occur when the horizontal line touches the SBFAD for L_r=0.6. Subsequent crack growth leads to increasing L_r and decreasing K_{mat}, and a locus of points are generated for increasing ε_r.

EXPERIMENTS AND RESULTS

To examine in more detail the applicability of the strain based approach results from CCG tests conducted on a simulated low alloy steel HAZ material at 380°C are explored in this section. The details of the tests and their results are given in [16]. The test programme used compact tension specimens subjected to constant load with the total displacements monitored throughout each test. Tests lasted from about 40 hours up to 1000 hours. In all tests there was very limited evidence of plasticity before the onset of creep.

In the absence of plasticity it is important to determine the elastic and creep displacements which can be separated by displacement partitioning presented earlier by Saxena and Landes [17]. At a given crack length the total displacement, Δ_t, is the sum of the elastic, Δ_e, and the creep, Δ_c, displacement, where

$$\Delta_t[a] = \Delta_e[a] + \Delta_c[a] \tag{4}$$

As the crack length, a, increases the elastic displacement is estimated using

$$\Delta_e[a] = \Delta_e[a_o] \frac{C_e[a]}{C_e[a_o]} \tag{5}$$

where C_e is the elastic compliance function and $\Delta_e[a_o]$ is the measured initial elastic displacement at the initial crack length, a_o. For the CT specimen the elastic compliance $C_e(a/W)$ expressed as a function of the normalised crack length, a/W [18] is:

$$C_e\left[\left(\frac{a}{W}\right)\right] = \frac{1}{EB}\left(\frac{1+(a/W)}{1-(a/W)}\right)^2\left[\begin{matrix}2.163+12.219(a/W)-20.065(a/W)^2\\-0.9925(a/W)^3+20.609(a/W)^4-9.9314(a/W)^5\end{matrix}\right] \tag{6}$$

The elastic displacement can therefore be determined for a growing crack using equation (5). The creep displacement is determined from

$$\Delta_c[a] = \Delta_T[a] - \Delta_e[a] \qquad (7)$$

Overall, the extent of cracking for all the tests was between 4 and 10 mm. This is very extensive compared to conventional ductile crack growth (tearing) tests. The calculated creep displacements using eqn 7 are shown in figure 2. For some tests (C, E and H) there is a consistent increase in creep displacement with increasing time. However, for other tests particularly for $t/t_f > 0.3$, where t_f is the failure time of the specimen, the estimated creep displacement decreased with increasing time.
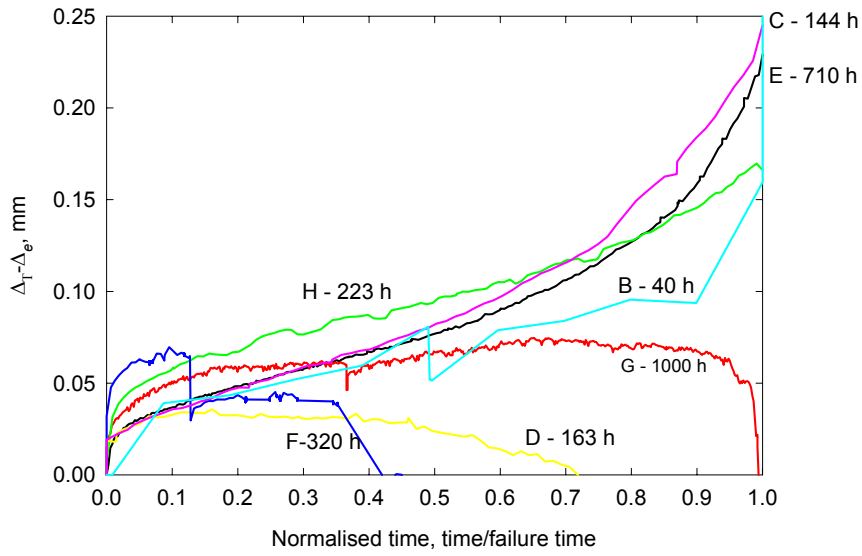

Figure 2, Total Displacement - elastic displacement for simulated HAZ material

In creep-brittle materials, the amount of creep deformation represents a very small percentage of the total displacement. Therefore, in the absence of plasticity the change of displacement caused by a change in elastic compliance is comparable to the total displacement. Consequently small errors in estimating the extent of cracking would lead to large errors in determining creep displacements. Tests D, F and G yielded negative apparent creep displacements. In these tests it is not possible to characterise CCG using C^*.

An alternative approach is to examine CCG in terms of material resistance. For ductile tearing involving rate independent processes the J-resistance curve has been adopted as a measure of a material's resistance to ductile crack growth. This approach is explored here. In general the total energy dissipated, during each test, can be determined from the sum of elastic, plastic and creep displacements. In order to determine the total J_T the elastic, plastic and creep terms were determined using the conventional J formulae, where,

$$J_T = J_e + J_p + J_c \qquad (8)$$

with

$$J_e = \frac{K^2(1-v^2)}{E}; J_p = \frac{\eta U_p}{B(W - a_o)}; J_c = \frac{\eta U_c}{B(W - a_o)} \qquad (9)$$

where η is a geometric factor, a_o is the initial crack length, and U_p and U_c are the areas under the plastic and creep parts of the load line displacement curves obtained from the experiments. To determine J_T from the creep crack growth tests it was necessary to obtain from the experiments not only the creep displacements but also the elastic and plastic displacements during initial load up. As

noted earlier the total displacements in the simulated HAZ material were dominated by elastic and creep displacements.

Material resistance curves derived using J_T are shown in figure 3. Each test generates a separate R-curve, with creep tests of short duration giving an R-curve which is generally higher than an R-curve for longer duration. From these results a measure of the material resistance for a given crack extension can be obtained as a function of time. This will be explored in later work.
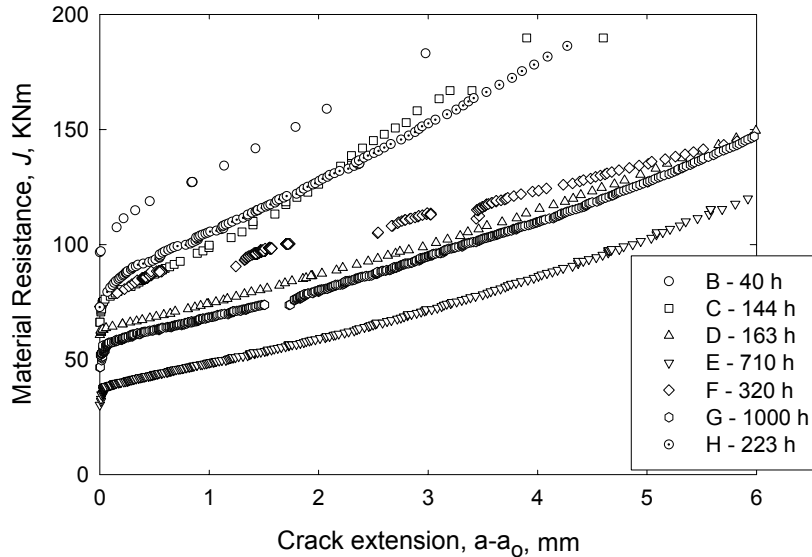

Figure 3, Resistance Curves for Simulated HAZ material

ASSESSMENT OF EXPERIMENTS USING THE SBFAD

In this section the results of the CCG tests on the simulated low alloy steel HAZ are assessed using the strain based failure assessment diagram (SBFAD). In each case K_r was determined using

$$K_r = \sqrt{\frac{K^2 / E'}{J_T}}$$

(10)

where J_T has been obtained using the measured value for the elastic and creep displacements, using eqn 8. The rate ε_r has been obtained from eqn 3.

Figure 4 shows results from test E. A curve for K_r as a function of ε_r obtained from the experiment is shown. As the test progressed K_r decreased and ε_r increased. The position on the curve corresponding to crack initiation is shown on the curve. Also shown are two loci obtained from eqn 2. One locus is for L_r=0.52, corresponding to the initial applied load, assuming plane strain conditions and using the 0.2% yield strength from high temperature tensile test. The second locus is for variable L_r, where L_r was determined accounting for crack growth. The differences between the two loci are largest towards the end of the test. The experimental result closely follows the predicted strain based failure assessment curve given by eqn 2. It is also evident that there was a period of creep strain accumulation prior to crack initiation. Initiation occurred when the experimental curve crossed the assessment line. This is also illustrated schematically in figure 1. Subsequent crack growth occurred such that the experimental curve essentially followed the assessment line.
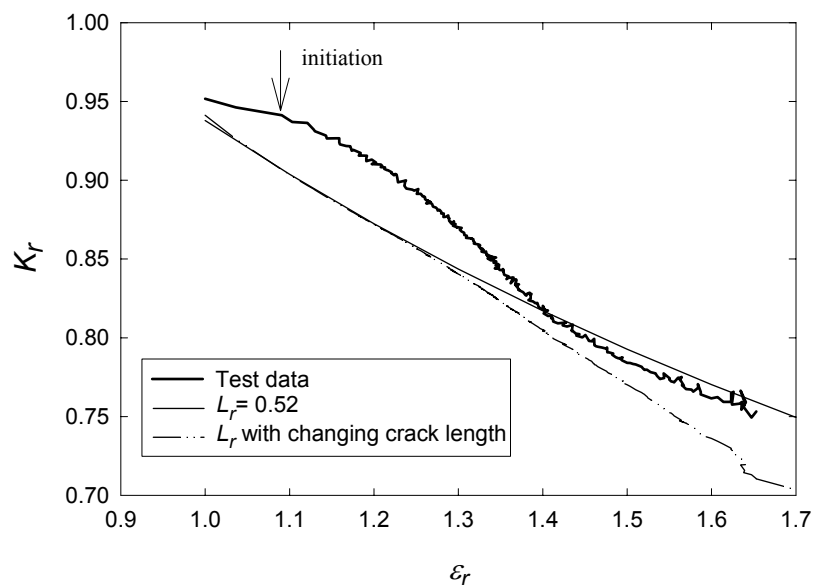
Figure 4, SBFAD assessments for simulatd HAZ material

CONCLUDING REMARKS

An alternative approach to characterising CCG using C^* has been proposed. The SBFAD provides a method of assessing the deformation throughout an entire test. The method uses the total accumulated material toughness and not the instantaneous creep rate to estimate the fracture parameter C^*. Experimental results for a creep-brittle simulated HAZ material have been used to demonstrate the principles of this new method.

REFERENCES

1. Gooch, D. J. and Kimmins, S. T. (1986). Journal of Strain Analysis. 21, 4, 231-242.
2. Webster, G.A. and Ainsworth, R.A. (1994). Chapman and Hall.
3. Ainsworth, R. A., Chell, G., Coleman, M. C., Goodall, W., Gooch, D. J., Haigh, J. R., Kimmins, S. T. and Neate, G. J. (1987). Fat. Fract. Eng. Mat. and Struct. 10, 2, 115-127.
4. ASTM E1457-92. (1996). ASTM 03.01, pp. 932-940.
5. Schwable, K-H., Ainsworth, R.A., Saxena, A. and Yokobori, T. (1999). Eng. Fract. Mech., 62, 1, 123-142.
6. Saxena, A. (1986). Fracture Mechanics-17, ASTM STP 905, pp. 185-201.
7. Tabuchi, M., Kubo, K., Yagi, K., Yokobori, Jr., A.T. and Fuji, A. (1999). Eng. Fract. Mech., 62, 1, 47-60.
8. Yokobori A.T. (1999). Eng. Fract. Mech., 62, 1, 61-78.
9. Yokobori A.T. (1998). Mat. at High Temp. 15, 2, 45-50.
10. Laiarinandrasana, L., Polvora, J.P., Piques, R. and Martelet, B. (1998). Mat. at High Temp. 15, 3/4, 181-186.
11. Bensussan, P., Piques, R. and Pineau, A. (1989). Non. Fract. Eng. ASTM STP 995, pp. 27-54. Saxena, A., Landes, J.D. and Bassani, J.L. (Eds). ASTM, Philadelphia.
12. Milne, I., Ainsworth, R.A., Dowling, A.R. and Stewart, S.T. (1988). Int. J. PVP, 32, 3-104.
13. Ainsworth, R. A. (1993). Fat. Fract. Eng. Mat. and Struct. 16, 10, 1091-1108.
14. Smith, D.J., Fookes, A.J., Dean, D.W. and Lamb, M. (1998). International Conference on Integrity of High Temperature Welds. pp. 355-370.
15. Kumar, V., German, M.D. and Shih, C.F. (1981). EPRI Report NP-5596, Electric Power Research Institute, Palo Alto, C.A.
16. Lamb, M. and Gladwin, D. N. (1998). BNFL, Magnox Generation, Confidential Report, M/TE/SXA/REP/0112/98.
17. Saxena, A. and Landes, J. D. (1984). Advances in Fracture Research, ICF-6, Pergamon Press, pp. 3977-3988.
18. Anderson,T.L. (1995). Fracture mechanics – Fundamental and Application. CRC Press, pp. 607.